SBS 0335–052W – AN EXTREMELY LOW METALLICITY DWARF GALAXY¹

Valentin A. Lipovetsky^{2,3}

Special Astrophysical Observatory, Russian Academy of Sciences, Nizhny Arkhyz, Karachai-Circessia 357147, Russia Electronic mail: val@sao.ru

and

Frederic H. Chaffee

W. M. Keck Observatory, 65-1120 Mamalahoa Hwy., Kamuela, HI 96743 Electronic mail: fchaffee@keck.hawaii.edu

and

Yuri I. Izotov²

Main Astronomical Observatory, Ukrainian National Academy of Sciences, Goloseevo, Kiev 252650, Ukraine Electronic mail: izotov@mao.kiev.ua

and

Craig B. Foltz

Multiple Mirror Telescope Observatory, University of Arizona, Tucson, AZ 85721 Electronic mail: cfoltz@as.arizona.edu

and

Alexei Y. Kniazev²

Special Astrophysical Observatory, Russian Academy of Sciences, Nizhny Arkhyz, Karachai-Circessia 357147, Russia

Electronic mail: akn@sao.ru

and

Ulrich Hopp⁴

Universitäts-Sternwarte, Scheiner Str. 1, D-81679, Munich, Germany Electronic mail: hopp@usm.uni-muenchen.de

³Deceased 1996.

¹Some of the observations reported here were obtained at the Multiple Mirror Telescope Observatory, a joint facility of the Smithsonian Institution and the University of Arizona, and at the W. M. Keck Observatory (WMKO), which is operated jointly by the California Institute of Technology, the University of California, and NASA. WMKO was made possible by the generous support of the W. M. Keck Foundation.

²Visiting astronomer, National Optical Astronomical Observatories.

⁴Visiting astronomer, Calar Alto German-Spain Observatory.

ABSTRACT

We present Multiple Mirror Telescope (MMT) and Keck II telescope spectrophotometry and 3.5m Calar Alto telescope R, I photometry of the western component of the extremely low-metallicity blue compact galaxy SBS 0335–052. The components, separated by 22 kpc, appear to be members of a unique, physically connected system. It is shown that SBS 0335–052W consists of at least three stellar clusters and has the same redshift as SBS 0335–052. The oxygen abundance in its two brightest knots is extremely low, 12 + log (O/H) = 7.22\pm0.03 and 7.13\pm0.08, respectively. These values are lower than in SBS 0335–052 and are nearly the same as those in I Zw 18. The (R - I) color profiles are very blue in both galaxies due to the combined effects of ionized gas and a young stellar population emission. We argue that SBS 0335–052W is likely to be a nearby, young dwarf galaxy.

Subject headings: galaxies: abundances — galaxies: irregular — galaxies: photometry — galaxies: evolution — galaxies: formation — galaxies: ISM — HII regions — ISM: abundances

1. Introduction

Since its discovery as an extremely low-metallicity galaxy, the blue compact galaxy (BCG) SBS 0335–052 (SBS – Second Byurakan Survey) has been seen as a good candidate to be a nearby, young dwarf galaxy (Izotov et al. 1990). This chemically-unevolved galaxy with oxygen abundance 1/40 the solar value (Terlevich et al. 1992; Melnick, Heydary-Malayeri & Leisy 1992; Izotov et al. 1997) is the second most metal-deficient BCG known, after I Zw 18, with an oxygen abundance of 1/50 (O/H) $_{\odot}$ (Skillman & Kennicutt 1993, hereafter SK93).

New evidence in favor of the evolutionary youth of SBS 0335–052 has been found in subsequent studies. Hubble Space Telescope (HST) V, I imaging of this galaxy (Thuan, Izotov & Lipovetsky 1997, hereafter TIL97) revealed blue (V - I) colors not only in the region of current star formation, but also in the 4 kpc diameter extended, low-intensity envelope. The emission from the underlying component, with (V - I) = 0.0-0.2, would seem to arise from the combination of ionized gas emission and emission from young ($\leq 10^8$ yr) stars (Izotov et al. 1997).

Another piece of evidence favoring of a young age for SBS 0335–052 has been presented by Thuan & Izotov (1997) from *HST UV* spectrophotometry. They have shown that this galaxy is a damped Ly α system with extremely high neutral hydrogen column density $N(\text{H I}) = 7 \times 10^{21} \text{cm}^{-2}$ suggesting a large amount of unprocessed neutral gas around the galaxy. The heavy element abundances in neutral gas are several orders of magnitude lower than those in the ionized gas (Thuan & Izotov 1997).

The Very Large Array (VLA) map of SBS 0335–052 reveals the presence at the same redshift of a large extended H I cloud, 64 kpc in size, with a mass two orders of magnitude larger than that of the observed stars (Pustilnik et al. 1998). Two prominent, slightly-resolved H I peaks have been detected, separated by 22 kpc. The eastern peak coincides approximately with SBS 0335–052. Pustilnik et al. (1997) sought to identify the western H I peak using the Digital Sky Survey (DSS) and found an optical counterpart designated as SBS 0335–052W. The redshift of this faint, slightly elongated compact galaxy, derived from a 6m telescope optical spectrum, is close to that of SBS 0335–052, suggesting that these two galaxies and the H I cloud form a common system.

The [N II] and [S II] lines in SBS 0335–052W were

too weak to be detected by Pustilnik et al. (1997) who concluded that this object may be a low-metallicity young galaxy. However, this conclusion is based on a low S/N spectrum in the $\lambda\lambda 4800-7200$ Å spectral range, so that the oxygen abundance was not derived. In this paper we present new MMT and Keck II spectrophotometric observations and 3.5m Calar Alto telescope CCD R, I photometry, derive for the first time the element abundances and obtain R, I and (R - I) profiles for SBS 0335–052W.

2. OBSERVATIONS

2.1. Optical spectroscopy

The MMT optical spectra of SBS 0335–052W were obtained on 1996 January 19 with the Red Channel of the MMT Spectrograph. We used a $1'' \times 180''$ slit; the 300 g mm⁻¹ grating provides a dispersion of 3 Å $pixel^{-1}$ and spectral resolution of about 10 Å in first order. To avoid second-order contamination, an L-38 blocking filter was used. The total spectral range was $\lambda\lambda 3700-7300$ Å. The spectra were rebinned by a factor of 2 along the spatial axis, hence, the spatial sampling was $0^{\prime\prime}_{..}6$ pixel⁻¹. The linear scale is $1^{\prime\prime}_{..}$ = 263 pc at the distance to SBS 0335-052W of 54.1 Mpc^5 . The total exposure time was 60 min, broken to three exposures of 20 min. The slit was oriented north-south ($PA=0^{\circ}$). The seeing during the observations was ~ 0.8 and the galaxy was observed at the airmass of 1.25. The standard star PG 0205+134 was observed for absolute flux calibration. Spectra of He-Ne–Ar comparison lamps were obtained before and after each observation to provide wavelength calibration.

The Keck II telescope optical spectra of SBS 0335– 052W were obtained on 1997 November 10 with the Low Resolution Imaging Spectrometer (LRIS; Oke et al. 1995), using the 600 g mm⁻¹ grating which provides a dispersion 1.28 Å pixel⁻¹ and a spectral resolution of about 4 Å in first order. The total spectral range covered was $\lambda\lambda 4100-6800$ Å. The 1"×180" slit was aligned along the SBS 0335–052W major axis with a position angle P.A. = -80°. No binning along the spatial axis has been done, yielding a spatial sampling of 0".2 pixel⁻¹. The total exposure time was 90 min, broken to three exposures of 30 min. The seeing during the observations was around 0".6 and the

⁵Hubble constant H_0 =75 km s⁻¹ Mpc⁻¹ is used throughout the text.

galaxy was observed at the airmass of 1.25. The standard star GD 50 was observed to obtain an absolute flux calibration. A Ne–Ar comparison spectrum lamp was obtained after the observation to facilitate wavelength calibration.

The data reduction was carried out at the NOAO headquarters in Tucson using the IRAF⁶ software package. Procedures included bias subtraction, cosmicray removal and flat-field correction using exposures of a quartz incandescent lamp. After wavelength mapping and night sky background subtraction each frame was corrected for atmospheric extinction and flux calibrated. The one-dimensional spectra were extracted from each flux-calibrated frame using the APALL routine. The extracted spectra were then coadded, not combined. The cosmic rays hits have been removed manually. To derive the sensitivity curves, we have fitted the observed spectral energy distributions of the standard stars with a high-order polynomial. The r.m.s. of the sensitivity response curve around the fit was $\sim 2\%$ and $\sim 1\%$ (in linear scale) during MMT and Keck II telescope observations respectively.

The MMT spectrum of the brightest $1'' \times 2''$ region of SBS 0335-052W is shown in Figure 1. The twodimensional spectrum obtained with LRIS along the major axis of SBS 0335–052W shows the presence of three emitting regions with the brightest region at the NW side of the galaxy and two fainter in the SE regions. One-dimensional spectra of each region in apertures $1'' \times 2''$ each are shown in Figure 2. In Figure 3 we show the spatial distribution of the observed flux and equivalent width of $H\alpha$ emission line. The location of regions with spectra presented in Figure 2 is shown by vertical lines. While in the MMT spectrum the [O III] $\lambda 4363$ emission line is barely detected and is blended with the strong $H\gamma$ emission line, it is evidently present in the LRIS spectra of two regions which allows the reliable determination of the electron temperature and element abundances.

In Table 1, the observed line intensities and intensities corrected for interstellar extinction for SBS 0335–052W are shown together with the extinction coefficient $C(\text{H}\beta)$, observed flux of the H β emission line, the equivalent width $EW(\text{H}\beta)$ and absorption

equivalent width EW(abs) of Balmer hydrogen lines. We show 1σ upper intensity limits for the lines which have not been detected. To correct for extinction we used the Galactic reddening law of Whitford (1958). The line intensity errors listed in Table 1 take into account the noise statistics in the continuum which implicitly includes the uncertainties of the data reduction (flat-field correction, sky subtraction), the errors in fitting of the sensitivity response curves and the errors in placing the continuum and fitting the line profiles with gaussians. These errors have been propagated to calculate element abundances. The line intensities in the brightest knot derived from the MMT and Keck observations are in general agreement implying the correctness of the measurements despite the difference in slit PA between them.

To derive the element abundances in SBS 0335-052W we adopted a two-zone photoionized H II region model (Stasińska 1990). The electron temperature, $T_e(O \text{ III})$, is derived from the [O III] $\lambda 4363/(\lambda 4959)$ + 5007) line intensity ratio using a five-level atom model, and the electron temperature $T_e(O \text{ II})$ from the relation between $T_e(O \text{ II})$ and $T_e(O \text{ III})$ fitted by Izotov, Thuan & Lipovetsky (1994, hereafter ITL94) for photoionized H II models by Stasińska (1990). The electron temperature for the S III ion is obtained using prescriptions by Garnett (1992). The electron number density N_e is derived from the [S II] $\lambda 6717$, 6731 lines. The values of $T_e(O \text{ III})$, $T_e(O \text{ II})$, $T_e(S \text{ III})$ III) and N_e (S II) are shown in Table 2. The ionic and total abundances are derived from Keck II telescope spectra as described by ITL94 and by Izotov, Thuan & Lipovetsky (1997, hereafter ITL97) and are shown in Table 2. However, due to the fact that these spectra cover a smaller spectral range, we use the intensities of the [O II] λ 3727, [Ne III] λ 3868 and [S II] λ 6717, 6731 emission lines in the MMT spectrum, scaled to the LRIS spectra, to derive oxygen, neon and sulfur abundances. The oxygen abundance in both of the brightest regions of SBS 0335–052W is 0.1–0.2 dex smaller than in SBS 0335-052 (Izotov et al. 1997) and is the same as that in I Zw 18 (SK93). The helium abundance derived from He I λ 4471 and λ 5876 emission line intensities is in agreement with He abundances in brighter blue compact galaxies (ITL94, ITL97). The abundances of other elements are close to the mean values for extremely metal-deficient galaxies (Thuan, Izotov & Lipovetsky 1995; Izotov et al. 1997; Izotov & Thuan 1998a).

⁶IRAF: the Image Reduction and Analysis Facility is distributed by the National Optical Astronomy Observatories, which is operated by the Association of Universities for Research in Astronomy, In. (AURA) under cooperative argeement with the National Science Foundation (NSF).

2.2. CCD photometry

The R,I photometric observations of SBS 0335–052W were obtained during the study of SBS 0335–052 with the prime focus CCD camera on the 3.5m telescope in Calar Alto on 1991 October 6. At f/3.5, with the GEC CCD 1152×770 pixels, (22.5 μ m pixel⁻¹), the field of view is 7.3×4.9 . Two exposures of 600 s and 900 s were taken in R and I, respectively. Two clusters, M92 and NGC 7790 were observed as photometric standards. The photometric calibration was made using the data of Christian et al. (1985). The observations were done under photometric conditions with a seeing of FWHM = 1.44 ± 0.11 and 1.22 ± 0.02 in R and I respectively. Airmasses were 1.45 for R and 1.46 for I.

All data reduction was done with MIDAS⁷. The frames were corrected for bias, dark, flat-field and, additionally, in the I passband, for fringe-pattern. Unfortunately, the fringe-pattern correction was not very good and there was some residual structure in both the horizontal and vertical directions as result of additional noise in the CCD readout. This structure was corrected by applying median filters separately in the X- and Y-directions.

Aperture photometry was performed on the standard star observations using the MAGNITUDE/CIRCLE task with the same aperture for all stars. The standard star measurements were used for the determination of the magnitude zero points and the transformation of the instrumental CCD magnitudes into the Johnson-Kron-Cousins RI system. For the standard stars, the comparison of the CCD and the catalogued magnitudes shows a scatter of $\sigma = 0.08$ mag for R and $\sigma = 0.12$ mag for I. No color term has been included in the transformation as tests revealed no significant color term was appropriate.

For the photometry of extended objects, we used the package SURFPHOT as well as dedicated software for adaptive filtering developed at the Astrophysical Institute of Potsdam (Lorenz et al. 1993). The adaptive filter allows one to reduce pixel noise by 3-4 times without loss of spatial resolution of bright cores of stars and galaxies and to retain the object's total flux as well. The smoothing scale of the adaptive filter was 11×11 pixels. Before applying an adaptive filter a special mask was built, where all bright stars and galaxies were masked out. Such a mask is necessary for proper determination of noise statistics used by the filter. The code used from the package for adaptive filtration for fitting of the sky background constructs the background within the masked regions, avoiding any polynomial approximation. Instead the algorithm of "stretched skin" is used, which iteratively fills the background inside the mask by interpolation of that from areas outside of the mask. Total magnitudes are $R = 19.03 \pm 0.09$ and $I = 19.08 \pm 0.14$ for SBS 0335–052W and $R = 16.57 \pm 0.08$ and $I = 16.92 \pm 0.12$ for SBS 0335–052. The total magnitude I for SBS 0335–052 is in a good agreement with total I = 16.88 from TIL97.

Elliptical fitting was performed with FIT/ELL3 in SURFPHOT package where isophotes of galaxies were fitted by ellipses and the deviations were analysed by means of Fourier techniques as is described by Bender & Moellenhoff (1987). To construct a surface brightness profile we used the effective radius as the geometrical average, $R_{eq} = \sqrt{ab}$. The brightness profile was decomposed into two components: a gaussian distribution in the central part and an exponential disk. For this, the FIT package was used. Weights in the fitting procedure were adopted as proportional to $1/\sigma$, where σ is the instrumental accuracy of the surface brightness profile.

The R images, isophotes and profiles with their decomposition for SBS 0335–052 and SBS 0335–052W are shown in Fig.4. The error bars for surface brightness profiles in both R and I bands are less than the symbol sizes. Therefore they are shown only on the (R - I) profiles. The error bar for the first point shows the accuracy of the transformation to the standard system. The error bars for the remaining points show the instrumental accuracy of the color and take into account the detector gain and photon statistics for each frame. The best linear fits to the outer parts of the R surface brightness distributions are given by

$$\mu_R = (21.25 \pm 0.05) + (2.03 \pm 0.02)r \tag{1}$$

for SBS $0335{-}052$ and

$$\mu_R = (22.22 \pm 0.12) + (1.60 \pm 0.07)r \qquad (2)$$

for SBS 0335–052W.

The corresponding exponential scale lengths in the R band are $\alpha_R = 535\pm5$ pc and $\alpha_R = 422\pm18$ pc for SBS 0335–052 and SBS 0335–052W respectively.

⁷MIDAS is an acronym for the European Southern Observatory package – Munich Image Data Analysis System.

3. DISCUSSION

The discovery of the new dwarf blue compact galaxy SBS 0335–052W poses several important questions: a) How is this galaxy related to the brighter, extremely low-metallicity galaxy SBS 0335–052? b) If this system of galaxies is physically connected, what is its evolutionary state? Is it an evolved system of galaxies, or are we observing a system of nearby young dwarf galaxies during their formation? c) If this system of galaxies is young, what kind of constraints should this impose for searches of primeval galaxies?

In Table 3 we show the general characteristics of SBS 0335–052 and SBS 0335–052W. Our determination of the heliocentric radial velocity for SBS 0335– 052W is in excellent agreement with the velocity of SBS 0335–052, and confirms the conclusion of Pustilnik et al. (1997) that SBS 0335–052 and SBS 0335– 052W are physically related and are two sites of star formation in the large cloud of neutral gas detected by Pustilnik et al. (1998) in their VLA observations. Therefore, we suggest that this system is probably at the very beginning of its evolution.

More evidence for a common evolution of the two H II regions in the SBS 0335–052 system comes from spectroscopic observations of SBS 0335–052W. The spectra of this H II region, shown in Figures 1 and 2, resemble a spectrum of more moderate excitation as compared with the spectrum of the brighter companion and shows stronger low excitation [O II] λ 3727 emission.

The age of ionizing stellar clusters can be estimated from the equivalent width of the $H\beta$ emission line. This age estimate may be subject to uncertainties introduced by the differences in spatial distribution of ionized gas and ionizing stellar clusters. Mindful of this possible source of uncertainty, the lower equivalent width of H β in SBS 0335–052W by factor of ~ 2 implies that its youngest ionizing stellar clusters are older by a few times 10^6 yr than those in SBS 0335-052. However, HST WFPC2 observations of SBS 0335–052 (TIL97, Papaderos et al. 1998) have shown the presence of several super-star clusters spanning in age the range from a few to several tens of Myr. The age of the oldest extended low-intensity stellar population in SBS 0335–052 is ~ 100 Myr (Izotov et al. 1997; TIL97). These observations imply that the assumption of an instantaneous burst of star formation is not valid. Instead, star formation in SBS 0335-052 during last ~ 100 Myr would be consistent

with propagating star formation from NW to SE at a velocity $\sim 18 \text{ km s}^{-1}$ in a region of $\sim 1 \text{ kpc}$ in size (Papaderos et al. 1998). A similar situation is observed in the other known very metal-deficient galaxy, I Zw 18, where star formation likely propagated in the SE direction from the older C component to the youngest SE component (Izotov & Thuan 1998b).

While the youngest ionizing cluster in the SBS 0335–052W seems to be older than that in the SBS 0335–052, the difference in oxygen abundance suggests that in general SBS 0335-052W might be younger than its brighter companion. The oxygen abundance in the two regions of SBS 0335–052W, $12 + \log (O/H) = 7.22\pm0.03$ and 7.13 ± 0.08 , is the lowest known for dwarf emission-line galaxies, and it is comparable with $12 + \log (O/H) = 7.17 - 7.26$ derived for I Zw 18 (SK93).

In Figure 4 we show the R, I and (R - I) profiles for both SBS 0335–052 and SBS 0335–052W obtained with the 3.5m telescope. The surface brightness distribution in I for SBS 0335–052 is in a good agreement with that obtained by TIL97 and the total Imagnitude derived from both observations is coincident within 0.05 mag. The R and I profiles for SBS 0335–052 and SBS 0335–052W at large distances are fitted well by an exponential. The (R - I) color in both HII regions gets redder with increasing radius. Izotov et al. (1997) have shown that the (V-I) color of the extended stellar emission is strongly modified by the emission of ionized gas. It is evident from Fig. 3b that the (R - I) color in SBS 0335-052W is affected by the presence of ionized gas emission but to a lesser extent than in SBS 0335–052 where gaseous emission is stronger. The R passband is more subject to the influence of gaseous emission due to the strong $H\alpha$ emission which reaches its maximum in the region 3".6 SE of the brightest part of the galaxy. In this region R is ~ 0.5 mag brighter due to the H α emission line contribution, while in the brightest region the brightening due to the presence of the H α emission is smaller, ~ 0.3 mag. However, the equivalent width of H α is small at distances r>3'' NW of the center of SBS 0335–052W and at distances r > 5''SE of the center (Fig. 3b). Therefore, corrections for gaseous emission in the outer part of SBS 0335-052W are small, not exceeding ~ 0.17 mag, and being even less than 0.1 mag in regions with $EW(H\alpha) \leq 200$ Å.

To derive the age of the extended stellar component in the SBS 0335–052W, we have calculated a grid of spectral energy distributions (SED) for stellar populations with ages between 10 Myr and 20 Gyr using isochrones of stellar parameters from Bertelli et al. (1994) for metallicities 1/20 of the solar value and the compilation of stellar atmosphere models from Lejeune, Cuisiner & Buser (1998). We adopt an initial mass function (IMF) with a slope -2.35, and lower and upper mass limits of $0.6M_{\odot}$ and $100M_{\odot}$, respectively.

The resulting calculated broad-band colors as a function of age of the stellar population produced during a single burst are shown in Table 4. The sharp change of (R - I) between 0.17 at log t=8.0 and 0.36 at log t=8.1 is caused by the appearance of the first asymptotic giant branch stars, where t is expressed in yr. The (V-I) and (V-K) colors are even more sensitive to the appearance of the first asymptotic giant branch stars and, therefore, they are better discriminators between young and old stellar populations.

It follows from Table 4 that the observed (R - I)= 0.2 in the outer envelope of SBS 0335-052W can be explained only by the presence of a stellar population with age ≤ 100 Myr. The assumption of a continuous star formation rate in the galaxy with an age ≤ 100 Myr does not change its colors appreciably due to the weak dependence of colors on age at t =10 - 100 Myr (Table 4) which is the most likely age for the extended stellar component in SBS 0335–052 and its western counterpart. Of course, we cannot exclude completely the presence of an old stellar population simply because the young stellar population dominates the radiation. However, if present, the extended old population in the SBS 0335-052 is less significant than in the majority of BCGs where it is easily detected. Hence, the R, I photometric results contradict neither the hypothesis of a young age for SBS 0335-052 and SBS 0335-052W, nor their common origin during the last ≤ 100 Myr. However, as the (R-I) color is a weak discriminator of the age of a stellar population, photometric observations in other broad bands are necessary to confirm this hypothesis.

The existence of two young regions of star formation separated by 24 kpc poses the problem of identifying a mechanism for synchronizing star formation. The velocity distribution of neutral gas in SBS 0335– 052 shows no jumps or discontinuities and resembles the velocity distribution in a rotating gaseous disk (Pustilnik et al. 1998). No stellar or ionized gaseous optical emission is detected between both the components (Papaderos et al. 1998). These observations argue against models where star formation in two widely separated regions is caused by the collision of two gaseous clouds or by tidal effects.

One plausible mechanism for synchronizing star formation in two widely separated regions could be the contraction of a protogalaxy. Adopting the number density of the neutral gas $\sim 0.1-1$ cm⁻³ from TIL97, we derive a free-fall time of ≤ 100 Myr, in agreement with our estimates of the age of the stellar population.

The SBS 0335–052 system has several similarities with the dwarf galaxy associated with the large H I cloud in Virgo (1225+01) discovered by Giovanelli & Haynes (1989). However, the SBS 0335–052 system is characterized by one order of magnitude larger luminosity and star formation rate. The H I distribution of 1225+01 shows two peaks separated by 15 arcmin, or 45 kpc, if a distance of 10 Mpc is adopted. The optical knots resembling H II regions coincide with one of the peaks; the other peak, however, has no optical counterpart. Salzer et al. (1991) presented a detailed optical imaging and spectroscopic study of the dwarf irregular galaxy located at the main peak of the H I cloud. They found that the entire galaxy is very blue. Nebular abundances derived from the spectroscopic data reveal that this object is relatively unevolved chemically, though it has an oxygen abundance 12 + $\log (O/H) = 7.66$, two to three times larger than in the SBS 0335–052 system. Furthermore, Salzer et al. found that only a tiny fraction (0.02% - 0.60%) of the mass in the NE H I clump of 1225+01 is in the form of stars. A similar value is found in the SBS 0335-052 system (Izotov et al. 1997). Based on the models of chemical and color evolution, Salzer et al. concluded that the galaxy associated with 1225+01 H I cloud is still undergoing formation and the stellar population of this galaxy is likely no older than roughly 1 Gyr.

If our conclusion about the youth of SBS 0335–052 is correct, we can compare properties of this young galaxy with theoretical predictions and properties of high-redshift galaxies which are often considered primeval. In SBS 0335–052, the Ly α emission line is not observed (TIL97, Thuan & Izotov 1997), contrary to theoretical predictions for young galaxies (Charlot & Fall 1993). The small mass, ~ $10^7 M_{\odot}$, of the older stellar population in SBS 0335–052 suggests that the star formation rate during the first 100 Myr is only 0.1–1 M_{\odot} yr⁻¹. During this period only 1% of gaseous mass is transformed to stars, contrary to predictions of several models of galaxy formation

(Meier 1976; Baron & White 1987; Lin & Murray 1992), where a significant part of the gas converts to stars during the collapse time. Probably, the formation of galaxies, or at least dwarf galaxies, is a more quiescent process with moderate conversion of gas into stars. We expect that a detailed study of the SBS 0335–052 system could provide constraints on models of galaxy formation and could provide useful guidelines with which to search for primeval galaxies at large redshifts.

V.A.L., Y.I.I. and A.Y.K. thank R. Green and the staff of NOAO for their kind hospitality. The authors are very grateful to Simon Pustilnik for stimulating discussions. Partial financial support for this international collaboration was made possible by INTAS collaborative research grant No 94–2285. U.H. acknowledges the support by the SFB 375 of the Deutsche Forschungsgemeinschaft. C.B.F. and F.H.C. acknowledge support from NSF grant AST 93-20715, for which they are very grateful.

REFERENCES

- Baron, E., & White, S. D. 1987, ApJ, 322, 585
- Bender, R., & Moellenhoff, C. 1987, A&A, 177, 71
- Bertelli, G., Bressan, A., Chiosi, C., Fagotto, F., & Nasi, E. 1994, A&AS, 106, 275

Charlot, S., & Fall, S. M. 1993, ApJ, 415, 580

- Christian, C. A., Adams, M., Barnes, J. V., Butcher, H., Hayes, D. S., Mould, J. R., & Siegel, M. 1985, PASP, 97, 363
- Garnett, D. R. 1992, AJ, 103, 1330
- Giovanelli, R., & Haynes, M. P. 1989, ApJ, 346, L5
- Izotov, Yu. I., Lipovetsky, V. A., Guseva, N. G., Kniazev, A. Yu., & Stepanian, J. A. 1990, Nature, 343, 238
- Izotov, Yu. I., Lipovetsky, V. A., Chaffee, F. H., Foltz, C. B., Guseva, N. G. & Kniazev, A. Yu. 1997, ApJ, 476, 698
- Izotov, Yu. I., & Thuan, T. X. 1998a, ApJ, 500, 188
- Izotov, Yu. I., & Thuan, T. X. 1998b, ApJ, 497, 227
- Izotov, Yu. I., Thuan, T. X., & Lipovetsky, V. A. 1994, ApJ, 435, 647 (ITL94)
- Izotov, Yu. I., Thuan, T. X., & Lipovetsky, V. A. 1997, ApJS, 108, 1 (ITL97)
- Lejeune, T., Cuisinier, F., & Buser, R. 1998, A&AS, 130, 65
- Lin, D. N. C., & Murray, S. D. 1992, ApJ, 394, 523 ¿
- Lorenz, H., Richter, G. M., Capaccioli, M., & Longo, G. 1993, A&A, 277, 321
- Meier, D. I. 1976, ApJ, 207, 343
- Melnick, J., Heydari-Malayeri, M., & Leisy, P. 1992, A&A, 253, 16
- Oke, J.B., Cohen, J.G., Carr, M., Cromer, J., Dingizian, A., Harris, F.H., Labrecque, S., Lucinio, R., Schall, W., Epps H., & Miller, J. 1995, PASP, 107, 375
- Papaderos, P., Izotov, Y. I., Fricke, K. J., Thuan, T. X., & Guseva, N. G. 1998, A&A, 338, 43
- Pustilnik, S. A., Lipovetsky, V. A., Izotov, Yu. I., Brinks, E., Thuan, T. X., Kniazev, A. Yu., Neizvestny, S. I., & Ugryumov, A. V. 1997, Pis'ma v A.Zh., 23, 350
- Pustilnik, S. A., Thuan, T. X., Brinks, E., Lipovetsky, V. A., & Izotov, Yu. I., 1998, in preparation

- Salzer, J. J., Alighieri, S. S., Matteucci, F., Giovanelli, R., & Haynes, M. P. 1991, AJ, 101, 1258
- Skillman, E., & Kennicutt, R. C., Jr. 1993, ApJ, 411, 655 (SK93)
- Stasińska, G. 1990, A&AS, 83, 501
- Terlevich, E., Terlevich, R., Skillman, E., Stepanian, J., & Lipovetsky, V. 1992, in Elements and Cosmos, eds.M.G.Edmunds, R.J.Terlevich (Cambridge: University Press), 21
- Thuan, T. X., Izotov, Yu. I., & Lipovetsky, V. A. 1995, ApJ, 445, 108
- Thuan, T. X., Izotov, Yu. I., & Lipovetsky, V. A. 1997, ApJ, 477, 661 (TIL97)
- Thuan, T. X., & Izotov, Yu. I. 1997, ApJ, 489, 623
- Whitford, A. E. 1958, AJ, 63, 201

This 2-column preprint was prepared with the AAS IATEX macros v4.0.

Fig. 1.— The observed spectrum of SBS 0335–052W obtained with Multiple Mirror Telescope in an $1'' \times 2''$ aperture.

Fig. 2.— The Keck II telescope spectra of three regions in SBS 0335–052W aligned in the direction from the SE (a) to the NW (c). All spectra have been extracted in the $1'' \times 2''$ apertures.

Fig. 3.— The spatial distribution of the observed flux (a) and equivalent width (b) of the H α emission line in $1'' \times 0''_{..}6$ apertures. The location of three regions with spectra displayed in Figure 2 are marked by vertical lines in Figure 3a. The linear scale is 1'' = 263 pc.

Fig. 4.— a) R-band images of SBS 0335–052 and SBS 0335–052W, obtained with the 3.5m Calar Alto telescope. North is up, East is left (scales as below); b) Isophotes in the R passband for SBS 0335–052 and SBS 0335–052W. The outermost isophote is 26 mag $\operatorname{arcsec}^{-2}$, the step is 0.5 mag $\operatorname{arcsec}^{-2}$, the linear scale is 1'' = 263 pc; c) The R, I and (R - I) profiles of SBS 0335-052 and SBS 0335-052W. The decomposition of R profiles on central starburst component and extended low surface brightness exponential profiles is shown by dotted lines. The error bars are shown only for the (R - I) profiles. The error bar for the first point shows the accuracy of the transformation to the standard system. The error bars for the rest points show the instrumental accuracy. The brighter galaxy is bluer in the central region, but the colors for both galaxies are the same in outer regions.

	Keck II				MMT		
Ion	Western knot		Eastern knot		Western knot		
	$F(\lambda)/F(\mathrm{H}eta)$	$I(\lambda)/I(\mathrm{H}eta)$	$F(\lambda)/F(\mathrm{H}eta)$	$I(\lambda)/I({ m H}eta)$	$F(\lambda)/F(\mathrm{H}eta)$	$I(\lambda)/I(\mathrm{H}eta$	
3727 [O II]					$0.652{\pm}0.027$	$0.698 {\pm} 0.03$	
3868 [Ne III]					$0.146 {\pm} 0.014$	$0.154{\pm}0.01$	
3889 He I + H8					$0.123 {\pm} 0.012$	$0.182 {\pm} 0.02$	
3968 [Ne III] + H7					$0.118 {\pm} 0.015$	$0.178 {\pm} 0.02$	
4101 $H\delta$	$0.177 {\pm} 0.005$	$0.254{\pm}0.008$	$0.200{\pm}0.012$	$0.219{\pm}0.016$	$0.197{\pm}0.013$	$0.250 {\pm} 0.02$	
$4340 \text{ H}\gamma$	$0.405 {\pm} 0.009$	$0.458 {\pm} 0.011$	$0.434{\pm}0.017$	$0.446{\pm}0.019$	$0.434{\pm}0.019$	$0.479 {\pm} 0.02$	
4363 [O III]	$0.036 {\pm} 0.002$	$0.035 {\pm} 0.002$	$0.044{\pm}0.007$	$0.043 {\pm} 0.007$	$< 0.05^{\rm a}$	< 0.05	
4471 He I	$0.037 {\pm} 0.002$	$0.036 {\pm} 0.002$	$0.040 {\pm} 0.007$	$0.040{\pm}0.007$	< 0.03	< 0.03	
4686 He II	< 0.01	< 0.01	< 0.02	< 0.02	< 0.03	< 0.03	
$4861 \text{ H}\beta$	$1.000 {\pm} 0.020$	$1.000 {\pm} 0.021$	$1.000 {\pm} 0.030$	$1.000 {\pm} 0.031$	$1.000 {\pm} 0.037$	1.000 ± 0.03	
4959 [O III]	$0.489 {\pm} 0.010$	$0.460 {\pm} 0.010$	$0.474{\pm}0.017$	$0.467 {\pm} 0.019$	$0.451{\pm}0.019$	$0.435 {\pm} 0.0$	
5007 [O III]	$1.452{\pm}0.028$	$1.366 {\pm} 0.028$	$1.379 {\pm} 0.040$	$1.358 {\pm} 0.040$	$1.308 {\pm} 0.047$	$1.259 {\pm} 0.0$	
5876 He I	$0.103 {\pm} 0.003$	$0.094{\pm}0.003$	$0.095{\pm}0.008$	$0.094{\pm}0.008$	$0.112{\pm}0.009$	$0.102 {\pm} 0.0$	
6300 [O I]	$0.015 {\pm} 0.002$	$0.013 {\pm} 0.002$	$0.017 {\pm} 0.004$	$0.017 {\pm} 0.004$	< 0.02	< 0.02	
6312 [S III]	$0.006 {\pm} 0.002$	$0.005 {\pm} 0.002$	< 0.02	< 0.02	< 0.02	< 0.02	
$6563 \ \mathrm{H}\alpha$	$3.069 {\pm} 0.059$	$2.769 {\pm} 0.061$	$2.720{\pm}0.073$	$2.685 {\pm} 0.079$	$3.129{\pm}0.107$	$2.759 {\pm} 0.1$	
6583 [N II]	$0.025 {\pm} 0.002$	$0.022 {\pm} 0.002$	$0.022{\pm}0.006$	$0.022 {\pm} 0.006$	^b		
6678 He I					< 0.03	< 0.03	
6717 [S II]					$0.071 {\pm} 0.008$	$0.062 {\pm} 0.0$	
6731 [S II]					$0.049 {\pm} 0.006$	0.043 ± 0.0	
$C(\mathrm{H}\beta) \mathrm{dex}$	$0.075 {\pm} 0.025$		$0.000 {\pm} 0.035$		$0.135 {\pm} 0.044$		
$F(H\beta)^{c}$	$1.95{\pm}0.03$		$0.55 {\pm} 0.02$		$1.76 {\pm} 0.05$		
$EW(H\beta)$ Å	99:	± 1	140	$140{\pm}2$		$86{\pm}1$	
EW(abs) Å	$5.7{\pm}0.2$		$1.9{\pm}0.7$		$2.4{\pm}0.5$		

TABLE 1 EMISSION LINE INTENSITIES

^ablend with H γ λ 4340.

^bblend with H α λ 6563.

^cin units of 10^{-15} ergs s⁻¹cm⁻².

Property	Western knot	Eastern knot
$T_e(O \text{ III})(\mathbf{K})$	$17,200{\pm}600$	$19,\!300{\pm}1,\!900$
$T_e(O \text{ II})(K)$	$14,700{\pm}500$	$15,500 \pm 1,500$
$T_e(S \text{ III})(K)$	$16,000 \pm 500$	$17,700\pm1,600$
$N_e({ m S~II})({ m cm}^{-3})$	$10{\pm}10$	$10{\pm}10$
$O^{+}/H^{+}(\times 10^{5})^{b}$	0.60 ± 0.06	0.51 ± 0.13
$O^{++}/H^+(\times 10^5)$	1.08 ± 0.09	$0.85 \ \pm \ 0.20$
$O/H(\times 10^5)$	1.68 ± 0.11	1.35 ± 0.23
$12 + \log(O/H)$	7.22 ± 0.03	7.13 ± 0.07
$N^{+}/H^{+}(\times 10^{7})$	1.72 ± 0.17	1.52 ± 0.38
ICF(N)	2.81	2.67
$\log(N/O)$	$-1.54 \ \pm \ 0.07$	-1.53 ± 0.19
$Ne^{++}/H^{+}(\times 10^{5})^{b}$	0.24 ± 0.03	
ICF(Ne)	1.55	
$\log(Ne/O)$	$-0.65 \ \pm \ 0.07$	
${\rm S}^{+}/{\rm H}^{+}(\times 10^{7})^{\rm b}$	1.09 ± 0.11	
$S^{++}/H^+(\times 10^7)$	2.15 ± 0.64	
ICF(S)	1.29	
$\log(S/O)$	$-1.60 \ \pm \ 0.08$	
γ (He I λ 4471) ^c	0.002	0.004
$He^{+}/H^{+}(\lambda 4471)$	0.076 ± 0.005	0.086 ± 0.016
γ (He I λ 5876) ^c	0.004	0.005
$\mathrm{He^{+}/H^{+}}(\lambda5876)$	$0.078 {\pm} 0.002$	$0.080 {\pm} 0.007$
${\rm He^{++}/H^{+}}(\lambda4686)$	$< 10^{-4}$	$< 10^{-4}$
ICF(He)	1.000	1.000
He/H (weighted mean)	$0.078 {\pm} 0.002$	$0.081{\pm}0.006$
Y (weighted mean)	$0.238 {\pm} 0.007$	$0.244{\pm}0.020$

TABLE 2 Ionic and Total Element Abundances^a

^aAbundances are derived based on Keck II telescope spectra.

^bThe abundance is calculated from observed relative intensity of ion line derived from MMT spectrum.

 $^{\rm c}(1{+}\gamma)^{-1}$ is a correction factor for collisional enhancement of He I emission line.

Table 3 Observed and Derived Parameters for the SBS 0335–052 $$_{\rm SYSTEM}$$

Parameter	0335 - 052 W	0335-052
$\alpha(2000)$	$03^h 37^m 38^{s} 4$	$03^h 37^m 44 \stackrel{s}{.}0$
$\delta(2000)$	$-05^{\circ}02^{\prime}36^{\prime\prime}$	$-05^{\circ}02^{\prime}39^{\prime\prime}$
$R \operatorname{mag}^{\mathrm{a}}$	$19.03 {\pm} 0.09$	$16.57 {\pm} 0.08$
$R-I \mathrm{mag}^{\mathrm{a}}$	$-0.05 {\pm} 0.15$	$-0.35 {\pm} 0.14$
$V_{opt} \text{ km s}^{-1}$	4069 ± 20^{a}	4060 ± 12
$V_{\rm HI} \rm \ km \ s^{-1b}$	4017 ± 5	$4057 \pm\ 5$
$D \mathrm{Mpc}$	54.1	54.1
$M_R \operatorname{mag}$	-14.64	-17.10
$R_{26} \mathrm{~kpc}$	1.42	2.50

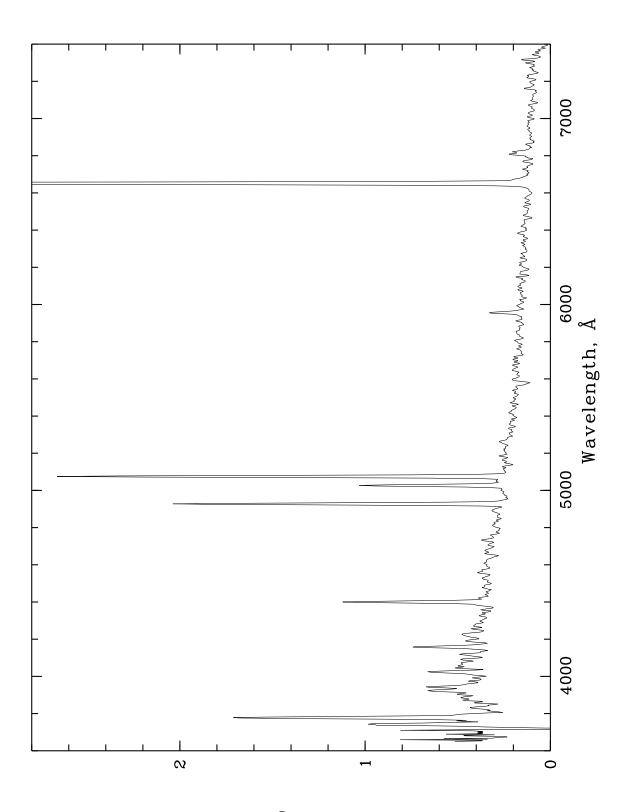
^aThis paper.

^bPustilnik et al. (1998).

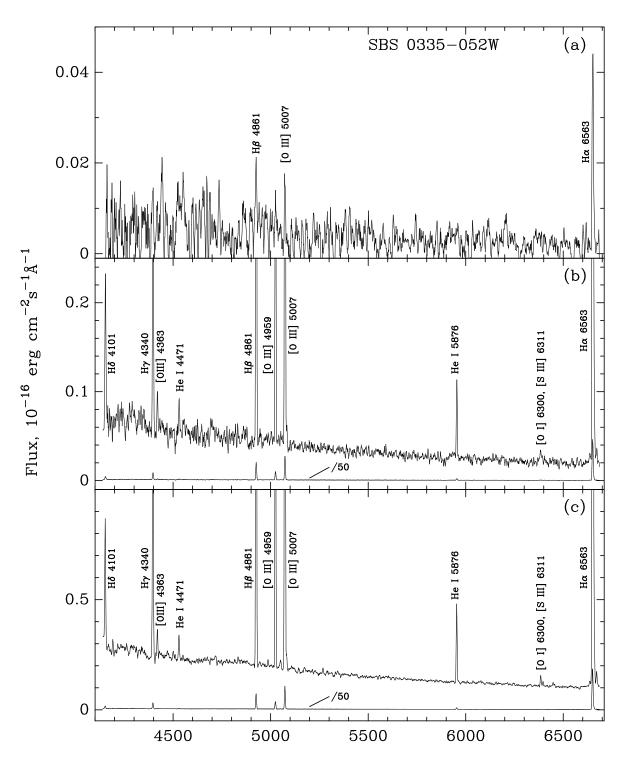
Table 4 Synthetic colors of single stellar population with $Z{=}Z_{\odot}/20$

$\log t^{\rm a}$	(U-B)	(B - V)	(V - I)	(R-I)	(V-K)
7.0	-1.00	-0.15	-0.03	-0.08	-0.31
7.5	-0.72	0.01	0.35	0.13	0.73
8.0	-0.49	0.07	0.43	0.17	0.83
8.1	-0.41	0.19	0.79	0.36	1.60
8.5	-0.25	0.23	0.83	0.38	1.66
10.0	-0.23	0.65	1.14	0.48	2.06

^aAge t is in yr.



Flux, 10⁻¹⁶erg s⁻¹cm^{-2Å-1}



Wavelength, Å

